Optical Materials 47 (2015) 244–250

Contents lists available at ScienceDirect

Optical Materials

journal homepage: www.elsevier.com/locate/optmat

# Electron Spin Resonance study of charge trapping in $\alpha$-$ZnMoO_4$ single crystal scintillator

M. Buryi [a,*], D.A. Spassky [b,c], J. Hybler [a], V. Laguta [a], M. Nikl [a]

[a] Institute of Physics AS CR, Cukrovarnicka 10, 162 00 Prague, Czech Republic
[b] Institute of Physics, University of Tartu, Ravila 14c, 50411 Tartu, Estonia
[c] Skobeltsyn Institute of Nuclear Physics, M.V. Lomonosov Moscow State University, Moscow 119991, Russia

ARTICLE INFO

*Article history:*
Received 19 February 2015
Received in revised form 6 May 2015
Accepted 19 May 2015
Available online 3 June 2015

*Keywords:*
Electron Spin Resonance
Scintillator
Charge traps
Zinc molybdate

ABSTRACT

The origin and properties of electron and hole traps simultaneously appearing in $\alpha$-$ZnMoO_4$ scintillator after X-ray irradiation at low temperatures ($T < 35$ K) were studied by Electron Spin Resonance (ESR). ESR spectrum of the electron type trap shows pronounced superhyperfine structure due to the interaction of electron spin with nuclear magnetic moments of $^{95,97}Mo$ and $^{67}Zn$ lattice nuclei. Considering the nearly tetragonal symmetry of the center this allows us to identify the electron trap as an electron self-trapped at the $(Mo(1)O_4)^{2-}$ complex. Nearly 60% reduction of the spin–orbit coupling at the Mo(1) ion is caused by the overlap of the Mo and ligand oxygen orbitals indicating an essential delocalization of the electron over the complex. Holes created by the X-ray irradiation form the $O^-$ type defects. Superhyperfine structure of their ESR spectra shows the contributions from two groups of $^{95,97}Mo$ nuclei and from $^{25}Mg$ nucleus as an uncontrolled impurity. It proves that namely the O(3) regular oxygen site is transformed into the $O^-$ center after the X-ray irradiation. Spectral parameters of the traps have been analyzed in the framework of the crystal field theory.

## 1. Introduction

Zinc molybdate, namely the $\alpha$-$ZnMoO_4$ insulator, has sufficiently high Mo mass concentration in the host and no other radioactive isotopes except the $^{100}Mo$. Consequently it fits the requirements for cryogenic phonon-scintillating detector applications [1]. However, the light yield of this material estimated at cryogenic temperatures shows an unexpectedly low value of 550 ph/MeV [2]. One of the reasons of the low light yield is the presence of shallow traps active at cryogenic temperatures. In the recent publication [2] these traps were identified as: (i) $(MoO_4)^{3-}$ complex created by an electron trapped at regular lattice $(MoO_4)^{2-}$ tetrahedron; (ii) $O^-$ defect created by a hole trapped at a regular lattice oxygen anion. Important role of the charge traps in the process of energy transfer was stressed. Preliminary Electron Spin Resonance (ESR) data of the mentioned defects are also provided in [2]. To the best of our knowledge, no other ESR study of the $ZnMoO_4$ has been reported so far and the actual structure and spectral parameters of these defects are not known. Low crystal symmetry of $ZnMoO_4$ (space group $P\bar{1}$) makes determination of correct spectral parameters complicated.

In preceding years many works were dedicated to the study of various irradiation-induced centers (charge traps) in promising scintillating materials such as $CaWO_4$, $CdWO_4$, $PbWO_4$ (PWO) [3–5], $ZnWO_4$ [6], aluminum perovskites ($YAlO_3$ (YAP) [7]) and garnets ($Y_3Al_5O_{12}$ (YAG), $Lu_3Al_5O_{12}$ (LuAG) as well as orthosilicates ($Y_2SiO_5$ (YSO) [8]). Their spectral parameters determined from ESR studies are summarized in [9]. The charge traps induced by irradiation of these materials were mostly $O^-$-like hole and $(WO_4)^{3-}$ and $(MoO_4)^{3-}$-like electron traps. Nevertheless it is worth noting the presence of the complex $(O–O)^{3-}$ hole defect in the $CdWO_4$ and $(WO_4–WO_4)^{3-}$, $(WO_3^-)_2^+$ (divacancy with one electron) and $(WO_3^-)_2^-$ (divacancy with three electrons) electron traps found in the $CaWO_4$ scintillators.

Electron and hole trap centers can be formed in a host due to the charge transfer and localization processes under sufficient irradiation dose. Charge carriers may become self-trapped at regular (unperturbed) lattice sites. The self-trapped holes (STH) studied in X-ray or $\gamma$-irradiated $CaWO_4$, UV irradiated $CdWO_4$, X-ray irradiated $ZnWO_4$ [6,9] were stable up to approximately 30–50 K. The STHs created in pure $Y_2SiO_5$ (YSO) [8] after X-ray irradiation, survived up to approximately 130 K and are gradually transformed into another, more stable $O^-$-like center. The $(WO_4)^{3-}$ polarons in UV irradiated $PbWO_4$ [3] and $Ti^{3+}$ polarons in $BaTiO_3$ [10] can

---

* Corresponding author.
*E-mail address:* buryi@fzu.cz (M. Buryi).

http://dx.doi.org/10.1016/j.optmat.2015.05.032
0925-3467/

be mentioned as an example of the self-trapped electrons (STE). These STEs are thermally stable up to about 40–70 K.

However, the most of the charge trapped centers are usually formed close to impurities, and/or vacancies in the lattice, which provide an additional stabilization of the centers. The electrons and holes trapped in such a way demonstrate higher thermal stability and survive at the trap to higher temperatures than the self-trapped charge carriers. For instance, $(WO_3)^-$ electron trap centers ($W^{5+}$ ions in the vicinity of $V_O$) in pure PWO [4] are stable up to room temperature. The $(MoO_4)^{3-}$ impurity complexes (electron trapped at $Mo^{6+}$ ion) in both doubly doped PWO:Mo,La and PWO:Mo,Y withstand heating up to 260 K [5]. One can thus infer that self-trapped charge carriers have activation energy much lower than those stabilized by an imperfection nearby. However, in general, it is not easy to distinguish the self-trapped mechanism of charge trapping from that involving a defect. Such a problem can be usually solved by performing the detailed study of local structure of charge trapping center.

In the present work we provide complete characterization of the $(MoO_4)^{3-}$ and $O^-$ defects created by X-ray irradiation at the cryogenic temperatures ($T < 35$ K) in the α-$ZnMoO_4$. Experimental data were analyzed in the framework of the crystal field theory that allowed to determine the parameters of electron-nuclei interactions in both types of defects and to clarify their local structures. Our data show that the $(MoO_4)^{3-}$ centers are created by the self-trapping mechanism while a hole additionally stabilized at $O^-$ ion by a Mg impurity ion.

## 2. Samples and experimental

Zinc molybdate studied in this paper belongs to the α-$ZnMoO_4$ structural type, space group $P\bar{1}$, triclinic system [11]. The unit cell is presented schematically in Fig. 1. It is composed of six $ZnMoO_4$ molecules. The lattice constants are $a_R = 9.625$ Å, $b_R = 6.965$ Å, $c_R = 8.373$ Å, $\alpha = 103.28°$, $\beta = 96.30°$, $\gamma = 106.72°$. The molybdenum atoms are surrounded by distorted oxygen tetrahedra creating three different types of Mo(1–3)$O_4$ complexes (see Fig. 1). Zinc atoms are embedded into the octahedral Zn(1) and Zn(2), and pentahedral Zn(3) positions (Fig. 1).

The zinc molybdate initial charge was prepared by a solid-phase synthesis technique from the $MoO_3$ and ZnO powders (both of 99.995% purity). Single crystals were grown in the frameworks of LUMINEU program from the stoichiometric melt by the low temperature gradient Czochralski technique. Since the crystallographic axes (marked as $a_R$, $b_R$, $c_R$ in Fig. 2) do not form the orthogonal basis needed for ESR measurements, the crystals were cut from the parent boule in three orthogonal planes (*ab*), (*bc*) and (*ac*) which essentially differ from the real lattice directions. In the choice of the orthogonal set of axes we took advantage of the cleavage plane existence. It is perpendicular to the vector *c* (reciprocal to the crystallographic vector $c_R$). Other two axes are located in the plane which is perpendicular to the *c* direction as it is shown in Fig. 2. Angular dependencies of ESR spectra were measured by rotation of samples with respect to these orthogonal axes. Continuous wave ESR measurements were carried out with standard 3 cm wavelength ESR spectrometer at 9.25–9.28 GHz within the temperature range 20–35 K using an Oxford Instruments cryostat. Samples were exposed to the X-ray irradiation directly in the spectrometer cavity at 30 K (this temperature is far below the traps stability threshold) for 30 min, using an X-ray tube ($U = 55$ kV, $I = 30$ mA).

## 3. Results and discussion

Prior to the X-ray irradiation there are no significant signals (Fig. 3) whereas strong resonance lines arise after the irradiation at 30 K earlier identified as belonged to an $O^-$ ion and $(MoO_4)^{3-}$ complex [2]. Both these paramagnetic centers will be considered in the detail separately.

### *3.1. Spectral characteristics and local structure of the $(MoO_4)^{3-}$ complex*

ESR spectrum corresponding to the molybdenum complex is shown in Fig. 4. The presence of hyperfine and superhyperfine (HF/SHF) structures beside the strong central line (nuclear spin $I = 0$) at the magnetic field value of 3517 G is clearly visible. The HF structure originates from the interaction of an electron spin with the nuclear magnetic moments of two intrinsic $^{95,97}Mo$ isotopes ($I = 5/2$), having nuclear moments ratio 0.98 and abundances of 15.92%, and 9.55%, respectively (blue sextet in Fig. 4). The group

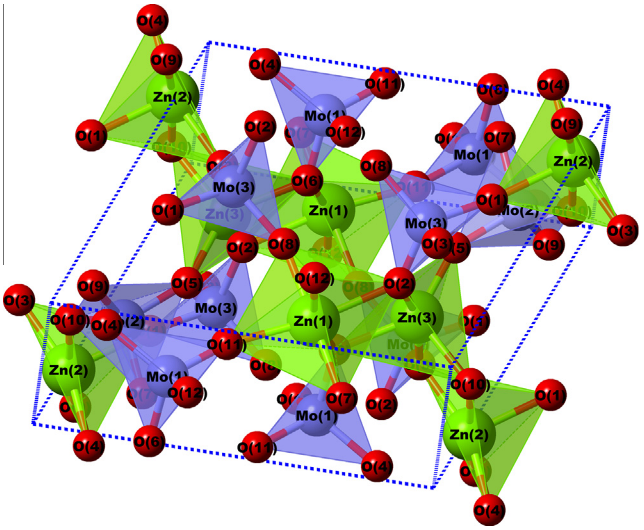

**Fig. 1.** Crystal structure of α-$ZnMoO_4$. Red balls represent oxygen ions and blue dashed lines enclose the margins of one unit cell. The data on the atom positions were taken from [11]. (For interpretation of the references to color in this figure legend, the reader is referred to the web version of this article.)

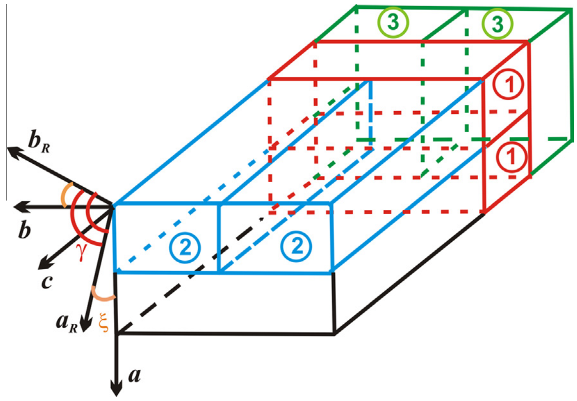

**Fig. 2.** Schematic view of how samples were cut from the as grown parent boule. The parallelepiped-shaped samples with specific faces orientation are distinguished by color as well as numbers assigning sample numbers; *a*, *b*, *c* are the virtual orthogonal axes used for sample rotations in ESR measurements; $\gamma = 107.25°$ is the angle in the real primitive cell between crystallographic directions $a_R$, $b_R$; $\xi = 2.5°$ is the deflection angle of *a* from $a_R$. *a*, *b*, $a_R$, $b_R$ are vectors which belong to the same plane. Vector *c* is reciprocal to the real $c_R$ (not shown in figure). (For interpretation of the references to color in this figure legend, the reader is referred to the web version of this article.)